TARANIS interacts with VRILLE and PDP1 to modulate the circadian transcriptional feedback mechanism in *Drosophila*

Abbreviated Title: Regulation of circadian rhythms by TARANIS

Oghenerukevwe Akpoghiran[1,2], Dinis J.S. Afonso[1,2], Yanan Zhang[1], and Kyunghee Koh[1*]

[1]Department of Neuroscience, the Farber Institute for Neurosciences, and Synaptic Biology Center, Thomas Jefferson University, Philadelphia, USA. 19107

[2]These authors contributed equally.

*Correspondence should be addressed to Kyunghee Koh at kyunghee.koh@jefferson.edu

Number of pages: 47 pages

Number of figures and tables: 7 figures and 3 tables

Number of words: Abstract = 222/250; Introduction = 629/650; Discussion = 1237/1500.

Conflict of Interest Statement: The authors declare no competing financial interests.

Acknowledgments: This work was supported by grants from the National Institutes of Health (R01NS086887 and R01NS109151 to K.K.). and funds from Thomas Jefferson University Synaptic Biology Center (to K.K.). We thank the Bloomington *Drosophila* Stock Center and National Institute of Genetics for fly stocks; *Drosophila* Genomics Research Center (supported by NIH grant 2P40OD010949-10A1) for vectors; Drs. Amita Sehgal, Paul Hardin, Justin Blau, and Jit Kong Cheong for antibodies and constructs; M. Boudinot and Dr. Francois Rouyer for the FaasX software; Luke Kim and William Wei for technical assistance; and Drs. Yohei Kirino, Joanna Chiu, Aaron Haeusler, Eun Young Kim, Sang Hyuk Lee, and James Jaynes, and members of the Koh lab for helpful discussions.

Abstract

The molecular clock that generates daily rhythms of behavior and physiology consists of interlocked transcription-translation feedback loops. In *Drosophila*, the primary feedback loop involving the CLOCK-CYCLE transcriptional activators and the PERIOD-TIMELESS transcriptional repressors is interlocked with a secondary loop involving VRILLE (VRI) and PAR DOMAIN PROTEIN 1 (PDP1), a repressor and activator of *Clock* transcription, respectively. Whereas extensive studies have found numerous transcriptional, translational, and post-translational modulators of the primary loop, relatively little is known about the secondary loop. In this study, we demonstrate that TARANIS (TARA), a *Drosophila* homolog of the TRIP-Br/SERTAD family of transcriptional coregulators, functions with VRI and PDP1 to modulate the circadian period and rhythm strength in *Drosophila*. Overexpression of TARA lengthens the circadian period, whereas *tara* mutants exhibit reduced rhythmicity, a faster molecular clock, and reduced expression of the PDF neuropeptide. We find that TARA can form a physical complex with VRI and PDP1, enhancing their repressor and activator functions, respectively. The conserved SERTA domain of TARA is required to regulate the transcriptional activity of VRI and PDP1, and its deletion leads to reduced locomotor rhythmicity. Consistent with TARA's role in enhancing VRI and PDP1 activity, overexpressing *tara* has a similar effect on the circadian period and rhythm strength as simultaneously overexpressing *vri* and *Pdp1*. Together, our results suggest that TARA modulates circadian behavior by enhancing the transcriptional activity of VRI and PDP1.

42 **Statement of Significance**

43 Internal molecular clocks generating circadian rhythms of around 24 hours broadly impact
44 behavior and physiology, and circadian dysfunction is associated with various neurological and
45 metabolic diseases. The *Drosophila* circadian clock is a valuable model for understanding the
46 molecular mechanisms underlying daily rhythms. In this study, we identify a conserved gene,
47 *taranis*, as a novel regulator of the *Drosophila* molecular clock. We show that TARANIS
48 modulates circadian behavior by physically interacting with and enhancing the transcriptional
49 activity of clock proteins VRILLE and PDP1. Since mammalian homologs of VRILLE and
50 PDP1 also function in the molecular clock, our results have implications for understanding the
51 mammalian circadian clock.

52 **Introduction**

53 The molecular mechanisms of endogenous circadian oscillators are conserved across
54 organisms, making *Drosophila melanogaster* a valuable model for understanding the genetics of
55 the circadian clock (reviewed in Allada and Chung, 2010; Hardin, 2011; Tataroglu and Emery,
56 2015; Patke et al., 2020). The molecular clocks in flies and mammals consist of interlocked
57 transcription-translation feedback loops that drive rhythmic gene expression. In the *Drosophila*
58 clock, the CLOCK-CYCLE (CLK-CYC) heterodimer binds to the E-box elements in the *period*
59 (*per*) and *timeless* (*tim*) promoters to activate their transcription (Allada et al., 1998), and the
60 PER-TIM heterodimer inhibits CLK-CYC, suppressing their own transcription (Hardin et al.,
61 1990). In an interlocked loop, CLK-CYC drives the transcription of *vri* and *Pdp1*. VRI and PDP1
62 competitively bind to the D-box elements in the *Clk* promoter to repress and activate *Clk*
63 transcription, respectively (Cyran et al., 2003; Glossop et al., 2003). The mammalian clock
64 involves analogous, although more complex, interlocked feedback loops, including nuclear
65 receptors and mammalian homologs of VRI and PDP1 (reviewed in Partch et al., 2014;
66 Takahashi, 2017; Patke et al., 2020). While many molecules underlying the transcriptional,
67 translational, and post-translational modulation of the primary feedback loop have been
68 identified (Allada and Chung, 2010; Zheng and Sehgal, 2012; Tataroglu and Emery, 2015; Patke
69 et al., 2020), the mechanisms regulating the secondary interlocked loop are less well understood
70 (Blau and Young, 1999; Cyran et al., 2003; Glossop et al., 2003; Benito et al., 2007; Zheng et al.,
71 2009; Ling et al., 2012; Gunawardhana and Hardin, 2017; Gunawardhana et al., 2021).

72 VRI and PDP1 are bZIP transcriptional factors essential for proper development and
73 circadian behavior (George and Terracol, 1997; Blau and Young, 1999; Reddy et al., 2000;
74 Cyran et al., 2003; Glossop et al., 2003). Both regulate the circadian output pathway and the

75 molecular clock. Null mutants of *vri* and *Pdp1* are lethal, but knocking down either gene in clock
76 neurons leads to arrhythmic behavior despite a functioning molecular clock, suggesting their role
77 in the clock output (Blau and Young, 1999; Cyran et al., 2003; Gunawardhana and Hardin,
78 2017). Additionally, *vri* overexpression substantially lengthens the circadian period (Blau and
79 Young, 1999), while an isoform-specific *vri* deletion mutant exhibits a shorter period
80 (Gunawardhana et al., 2021), indicating VRI's role in regulating the clock speed. An isoform-
81 specific, arrhythmic *Pdp1ε* mutant exhibits reduced CLK expression (Zheng et al., 2009),
82 demonstrating that PDP1 also functions in the molecular clock. Although PDP1 overexpression
83 has little effect on the period length (Zheng et al., 2009), heterozygous *Pdp1* null mutants show
84 slightly longer periods (Cyran et al., 2003), suggesting that PDP1 also modulates the clock
85 speed.

86 We previously reported that TARA interacts with Cyclin A (CycA) and Cyclin-
87 dependent kinase 1 (Cdk1) to promote sleep in *Drosophila* (Afonso et al., 2015b). In addition,
88 TARA and its mammalian homologs, Transcriptional Regulator Interacting with PHD-
89 Bromodomain (TRIP-Br, also known as SERTAD) family of proteins, function in diverse
90 biological processes, including cell cycle progression, metabolic regulation, and transcriptional
91 coregulation (Hsu et al., 2001; Calgaro et al., 2002; Liew et al., 2013; Dutta and Li, 2017).
92 TARA was initially categorized as a Trithorax group (TrxG) member of transcriptional
93 coactivators (Calgaro et al., 2002). However, a later study found that TARA enhances Polycomb
94 (Pc)-mediated transcriptional repression (Dutta and Li, 2017), suggesting that TARA may act as
95 a transcriptional coactivator or corepressor depending on the cellular context and interaction
96 partners. Here, we report a novel role of TARA in the transcriptional coregulation of VRI and
97 PDP1 in the molecular clock. Our results suggest that TARA modulates the pace of the

98 molecular clock and locomotor activity rhythms by physically interacting with and enhancing the
99 transcriptional activity of VRI and PDP1. Our study has implications for understanding the
100 mammalian circadian clock since mammalian homologs of VRI and PDP1 also function in the
101 molecular clock.
102
103 **Materials and Methods**
104 *Fly stocks*
105 Flies were raised on standard food containing molasses, cornmeal, and yeast at 25°C under 12 h-
106 12 h light-dark (LD) cycle. The following lines were obtained from the Bloomington *Drosophila*
107 Stock Center: UAS-*tara*-RNAi (JF01421, # 31634), UAS-*dicer2* (*dcr2,* #24650), *tara*^{1} (#6403),
108 UAS-*vri* (#78077), *elav-Gal4* (#458)*, nos-Cas9* (#54591), *tim-Gal4* (#80941), *Pdf-Gal4*
109 (#80939) and the background control line *iso31* (w^{1118}, #3605). The UAS-*tara*-RNAi (6889R-1,
110 #NM_080255.2) line was obtained from the National Institute of Genetics, Japan. UAS-*Pdp1*
111 and *tara*^{s132} were previously described (Zheng et al., 2009; Afonso et al., 2015b). UAS-*dcr2* was
112 combined with two RNAi lines (JF01421 and 6889R-1) to enhance the efficiency of *tara*
113 knockdown. TARA and its mammalian homologs have four conserved domains: CycA binding
114 homology (CAB), SERTA, PHD-Bromo binding (PBB), and C-terminal (Hirai et al.). UAS-*tara*
115 (containing the full-length *tara-B* coding sequence) and *tara* domain deletion (ΔCAB, ΔSERTA,
116 ΔPBB, and ΔCT) lines were generated in this study. All fly lines were outcrossed with *iso31* for
117 at least five generations, except for the UAS-*tara*-RNAi and *nos-Cas9* lines.
118
119 *Circadian assays*
120 To conduct the circadian assays, 3 to 5-day-old flies that had been entrained to an LD cycle at

121 25°C were placed individually in small glass tubes containing 5% sucrose and 2% agar. The
122 *Drosophila* Activity Monitoring System (Trikinetics) was used to record circadian locomotor
123 activity in constant darkness (DD). We employed the FaasX software (M. Boudinot and F.
124 Rouyer, Institute of Neurosciences Paris-Saclay, France) to calculate the circadian period and
125 rhythm strength of each fly. The software analyzes activity data collected in 30-min bins using
126 $\chi 2$ analysis to determine the period length and rhythm strength. Based on the rhythm strength
127 value, each fly was classified as arrhythmic (<25), weakly rhythmic (25-50), or rhythmic (>50).
128 All flies were included in the statistical analysis of rhythm strength, while the analysis of period
129 length excluded arrhythmic flies.
130
131 *Immunohistochemistry*
132 Following dissection, adult brains were fixed in 4% paraformaldehyde for 30 min at room
133 temperature. The samples were blocked in 1% bovine serum albumin (BSA) for PER and PDF
134 antibody staining. The primary and secondary antibodies were diluted in 0.1% BSA. The primary
135 antibodies utilized were anti-PER (rabbit 13.1 from the Sehgal lab, University of Pennsylvania)
136 at a dilution of 1:8000 and mouse anti-PDF (mouse C7s from the Developmental Studies
137 Hybridoma Bank) at a dilution of 1:2000. The secondary antibodies, Alexa Fluor 647 goat anti-
138 rabbit and Alexa Fluor 488 goat anti-mouse (Invitrogen) were used at a dilution of 1:1000. Both
139 primary and secondary antibodies were incubated overnight at 4°C, and images were captured
140 using a Leica SP8 confocal microscope.
141
142 *Plasmid constructs for cell-based assays*
143 *Actin-Clk, Actin-per, Actin-Gal4, per-enhanced luciferase* (*per-luc*) (Darlington et al., 1998), and

144 pUAST-V5 vector were obtained from the Sehgal lab (University of Pennsylvania). *Clk-luc* (~3
145 kb *Clk* promoter region fused to a *luciferase* cDNA; Cyran et al., 2003), UAS-*vri, and* CMV-
146 *vri::VP16* were obtained from the Blau lab (New York University). UAS-*Pdp1* was previously
147 described (Zheng et al., 2009). CMV-FLAG::*hTRIP-Br1* and CMV-FLAG::*hTRIP-Br2* were a
148 gift from Dr. Jit Kong Cheong (National University of Singapore). *Actin-Renilla luciferease*
149 (*rluc*) and CMV-*rluc* (Promega) were used to control for transfection efficiency.
150 A full-length, untagged UAS-*tara* construct was generated by PCR-amplifying the entire
151 *tara*-B coding region from *tara* cDNA and inserting it into the pUAST vector (Brand and
152 Perrimon, 1993). UAS-HA*::tara* constructs were generated by inserting the *tara-B* coding
153 region, amplified from the untagged UAS-*tara* construct, into the pTHW Gateway vector
154 (*Drosophila* Genomics Resource Center) containing the UAST promoter and N-terminal 3xHA
155 tag. The TARA-B residues removed in the deletion constructs are as follows: ΔCAB:1-26,
156 ΔSERTA: 432-479, ΔPBB: 722-739, and ΔCT: 893-912. pUAST-attB-V5::*tara* was generated
157 by inserting the *tara-B* coding region into the pUAST-attB-V5 vector, which is derived from the
158 pUAST-attB vector (*Drosophila* Genomics Resource Center) for N-terminal V5 tagging. CMV-
159 *tara* was generated by digesting UAS-*tara* with BglII and XbaI, and inserting the *tara-B* coding
160 sequence into the BamHI and XbaI sites in the pCDNA3 vector (Invitrogen). UAS-*Pdp1*::V5
161 was generated by digesting UAS-*Pdp1* (Zheng et al., 2009) with NotI and XhoI, and inserting the
162 *Pdp1* coding sequence into the corresponding sites in the pUAST-V5 vector, which is derived
163 from pUAST for C-terminal V5 tagging. UAS-*vri*::MYC was generated by inserting
164 the *vri* coding sequence, amplified from a UAS-*vri* construct (Cyran et al., 2003), into the
165 pTWM Gateway vector (*Drosophila* Genomics Resource Center). The constructs were validated
166 by sequencing (GENEWIZ).

167

168 *Luciferase-based transcription assay*

169 *Drosophila* S2 cells were cultured at 25°C in Schneider's Medium (Gibco), while HEK293 cells
170 were cultured at 37°C in DMEM Medium (Gibco). Both media were supplemented with 10%
171 heat-inactivated fetal bovine serum and 1% penicillin/streptomycin. Approximately 24 h prior to
172 transient transfection, 48-well plates were seeded with ~1.5 x 10^5 *Drosophila* S2 or HEK293
173 cells and maintained at their respective temperatures (25°C or 37°C). Transfections were
174 performed with Effectene Reagent (Qiagen) per the manufacturer's protocol. Transcriptional
175 activity was determined using the Dual Luciferase Assay Kit (Promega). Approximately 48 h
176 after transfection, cells were lysed in 1X Passive Lysis Buffer (PLB), and luciferase activity was
177 measured using the Luciferase Assay Reagent in Cytation 5 Luminometer (Biotek) following the
178 manufacturer's instructions.

179 For the PDP1- and VRI-dependent transcriptional assay, the following constructs were
180 transfected: *Clk-luc* (10 ng), *Actin-rluc* (10 ng), *Actin-Gal4* (70 ng), UAS-*Pdp1*::V5 (10 ng),
181 UAS-*vri*::MYC (35 ng), and UAS-HA*::tara* (1 ng, 5 ng, or 15 ng). An empty pUAST::V5 vector
182 was included to ensure an equal amount of total DNA (150 ng) in all conditions. For the CLK-
183 dependent transcriptional assays, the following constructs were used: *per-luc* (20 ng), *Actin-rluc*
184 (5 ng), *Actin-Gal4* (20 ng), *Actin-Clk* (1 ng), UAS-HA::*tara* (10 ng or 30 ng). Empty *pActin* and
185 pUAST::V5 vectors were used to control for the total DNA amounts (150 ng). For the PER-
186 dependent transcriptional assay, the following constructs were transfected: *per-luc* (20 ng),
187 *Actin-rluc* (15 ng), *Actin-Gal4* (20 ng), *Actin-Clk* (1 ng), *Actin-per* (2 ng, 5 ng, or 15 ng), and
188 UAS-HA*::tara* (30 ng). Empty *pActin* and pUAST::V5 vectors were used to control for the total
189 DNA amounts (150 ng). For the VRI::VP16-dependent transcriptional assay, the following

190 constructs were transfected: *Clk-luc* (10 ng), CMV-*rluc* (10 ng), *Actin-Gal4* (70 ng), CMV-
191 *vri::VP16* (5 ng), CMV-*tara* (10ng or 30ng), CMV-HA::ΔSERTA (30 ng), CMV-
192 FLAG*::hTRIP-Br1* (30 ng) , CMV-FLAG*::hTRIP-Br2* (30 ng), and the pCDNA3 vector to
193 control for the total DNA amount (125 ng).
194
195 *Western analysis and co-immunoprecipitation (co-IP)*
196 To examine the expression levels of transfected proteins, *Drosophila* S2 cell lysates were
197 collected approximately 48 h after transfection. Cells were lysed in 1X PLB to release
198 cytoplasmic proteins, while the insoluble fractions were treated with a sample buffer containing
199 sodium dodecyl sulfate (SDS) to release nucleic proteins. For the co-IP assay, ~3.2×10^6 S2 cells
200 were seeded in each well of a 6-well plate and transfected ~24 h after seeding. Around 48 h after
201 transfection, cells were harvested and lysed in 1X RIPA buffer supplemented with Protease
202 Inhibitor Cocktail (Sigma). The cell lysates were pre-cleaned with Dynabeads Protein G
203 (Invitrogen) to avoid non-specific binding. The pre-cleaned lysates were incubated with anti-V5-
204 conjugated magnetic beads (Medical & Biological Laboratories) overnight at 4°C. To elute the
205 protein complexes bound to the beads, 2X SDS with 5% β-mercaptoethanol was used. Western
206 blot analysis was performed as described (Wu et al., 2010). Antibodies against TARA (TJR51,
207 1:1000; Afonso et al., 2015b), HA (Covance, 1:1000), PDP1 (1:1000; Cyran et al., 2003), β-
208 ACTIN (Abcam, 1:8000), and Histone H3 (Abcam, 1:3000) were used.
209
210 *Generation of tara mutants with domain deletions and a UAS-tara transgenic line*
211 To identify an optimal protospacer adjacent motif (PAM) sequence within each domain, we
212 utilized the flyCRISPR target finder (https://flycrispr.org/target-finder). The following PAM

213 (shown in bold) and their corresponding flanking sequences were identified, with the numbers
214 indicating the nucleotide positions in the *tara-b* transcript: CAB domain: 552-574 – **CCA** AGC
215 GGA AGC ATG AGC TGA CC; SERTA domain: 1781-1802 – G CCA ACA GGA GTT GCT
216 ACA **AGG**; PBB domain: 2672-2680 – TA CTA GCG ATT CGG GTT ATG **CGG**; CT
217 domain: 3186-3208 – **CCC** GCC TGC ACG ACA ACG AAC TG. To introduce the domain-
218 specific protospacer sequences into the pCFD4 vector (Addgene), we employed the ligation-
219 independent Gibson Assembly method (NEBuilder, New England BioLabs) according to the
220 manufacturer's protocol. Transgenic flies carrying domain-specific gRNAs were generated using
221 the standard embryo injection technique (Rainbow Transgenics). Domain-specific deletions were
222 generated by crossing fly lines carrying the domain specific gRNAs with a *nos-Cas9* fly line.
223 Mutant flies were identified by sequencing the genomic DNA (GENEWIZ). Additionally, a
224 transgenic fly line carrying the untagged UAS-*tara* construct was generated using the standard
225 embryo injection technique (Rainbow Transgenics).
226
227 *RNA extraction and quantitative real-time PCR (qPCR)*
228 Total RNA was extracted from 30 male fly heads using 1 mL of TRIzol Reagent (Ambion). We
229 employed 100 µL of 1-Bromo-3-Chloropropane (Molecular Research Center, Inc.) to separate
230 the phases, and RNA precipitation was achieved by adding 500 µL of 2-propanol. After
231 treatment with 2 µL of DNaseI, cDNA was amplified from 1 µg of RNA using a high-capacity
232 cDNA Reverse Transcription Kit (Applied Biosystems). For qPCR, we used SYBR Green PCR
233 Master Mix (Applied Biosystems) and the 7500 Real-Time PCR System (Applied Biosystems). 3
234 technical replicates of 6 independent biological samples were assayed for each genotype. The

235 following primers were used for *Pdf*: 5'-CCT TGT GCT TCT GGC CAT TT-3' and 5'-GTC
236 GAG GAG ATC CCG ATT GT-3'. *actin* mRNA was used for normalization.
237
238 *Experimental design and statistical analyses*
239 Throughout the study, we employed a between-subject design. The experimental design is
240 visually depicted in the figures and described in the corresponding figure legends. Behavioral
241 experiments were repeated at least twice using flies from independent crosses, while cell-based
242 experiments were conducted at least three times. Statistical analyses were performed using
243 GraphPad Prism 9. For datasets with two groups, Welch's *t*-tests were utilized for comparisons.
244 To compare multiple groups, one-way Brown-Forsythe and Welch ANOVA tests were
245 conducted, followed by Dunnett's T3 multiple comparisons tests. For experiments involving two
246 factors, two-way ANOVA tests were employed, followed by Tukey's post hoc tests or Sidak's
247 multiple comparisons tests.

248 **Results**

249

250 **TARA functions in clock neurons to promote rhythmic behavior**

251 We previously showed that *tara* mutants display arrhythmic locomotor behavior as well
252 as reduced sleep (Afonso et al., 2015b). We confirmed that the reduced rhythmicity maps to the
253 *tara* locus using RNAi-mediated *tara* knockdown in all neurons using *elav-Gal4* (Table 1, Fig. 1
254 A,B). The *Drosophila* brain contains ~150 circadian neurons in several clusters. A cluster of
255 clock neurons expressing the Pigment Dispensing Factor (PDF) neuropeptide, called small
256 ventral lateral neurons (s-LN_vs), is essential for free-running rhythms in DD (Renn et al., 1999).
257 To examine where TARA functions to promote rhythmic behavior, we employed *tim-Gal4*,
258 which targets all clock neurons, and *Pdf-Gal4*, which targets the PDF-expressing LN_vs. Male
259 flies are typically used for assaying locomotor rhythms because they display more robust and
260 consistent rhythms than females. However, because pan-neuronal *tara* knockdown led to
261 lethality in males, female flies were used in the pan-neuronal knockdown experiment. Both
262 males and females were assayed in experiments using *tim-Gal4* and *Pdf-Gal4*.

263 In both males and females, knockdown of *tara* in all clock neurons using *tim-Gal4*
264 resulted in a significant reduction of rhythm strength (Table 1, Fig. 1). In contrast, restricted *tara*
265 knockdown in PDF-expressing LN_vs did not significantly affect circadian behavior. This finding
266 suggests that TARA functions in multiple clock neuron clusters to regulate rhythmic behavior.
267 Comparing female data with *elav-Gal4* vs. *tim-Gal4*, we observed that pan-neuronal knockdown
268 of *tara* had a more substantial effect on rhythm strength than knockdown in clock neurons (Table
269 1, Fig 1A,B), suggesting TARA also functions in non-clock neurons to promote rhythmic
270 locomotor activity. The period length remained largely unaffected by *tara* knockdown (Table 1,

271 Fig. 1). Our results suggest that TARA promotes rhythmic locomotion in clock and non-clock
272 neurons.
273
274 **TARA modulates the speed of the circadian clock**
275 To investigate whether TARA influences molecular clock oscillation, we examined PER
276 protein expression in s-LN_vs in DD. Although over 80% of *tara*$^{s132/1}$ mutants are arrhythmic or
277 weakly rhythmic (Afonso et al., 2015b), they displayed robust daily cycling of PER levels in DD
278 (Fig. 2A,B), suggesting that TARA plays a role in the circadian output pathway. Interestingly,
279 the pattern of PER cycling suggests that TARA also contributes to setting the pace of the
280 molecular clock. Compared to control brains, *tara* mutant brains exhibited a significantly lower
281 PER signal at CT 3 and a substantially higher PER signal at CT 15 (Fig. 2A,B), consistent with a
282 faster molecular clock. We previously reported that *tara*$^{s132/1}$ mutants, which have the most
283 severe reduction in *tara* levels among viable *tara* mutants, did not exhibit shorter periods in
284 locomotor behavior (Afonso et al., 2015b). This may be because the more strongly affected
285 mutants were arrhythmic, leaving only the less severely affected mutants for period length
286 measurements. In addition to the PER cycling changes, we observed that PDF levels at the dorsal
287 projections of the s-LN_vs were considerably lower in *tara* mutants than in control flies (Fig.
288 2C,D). We also found a significant reduction in the total levels of *Pdf* mRNA in *tara* mutants
289 compared to the controls (Fig. 2E). However, the reduction in PDF protein was more pronounced
290 than that of the *Pdf* transcripts, suggesting that TARA impacts PDF levels at both the
291 transcriptional and post-transcriptional levels. *Pdf* null mutants display decreased rhythmicity
292 and shorter periods (Renn et al., 1999), suggesting that reduced PDF levels in *tara* mutants
293 contribute to their behavioral and molecular phenotypes.

294 To further examine the effect of TARA levels on the speed of the circadian clock, we
295 examined whether flies overexpressing TARA exhibit the opposite pattern of PER cycling as
296 *tara* mutants. Indeed, TARA overexpression in PDF-expressing (PDF+) neurons led to a
297 significantly lower PER signal at CT 21, consistent with a slower molecular clock (Fig. 3A,B).
298 Furthermore, flies overexpressing TARA in PDF+ neurons exhibited a significantly longer
299 circadian period than control flies (Table 1, Fig. 3 C-E). Collectively, our data suggest that *tara*
300 plays a role in setting the pace of the molecular clock and regulating the circadian output
301 pathway.
302
303 **Evolutionarily conserved domains in TARA contribute to locomotor rhythmicity**
304 TARA and its mammalian homologs have four conserved domains: CycA binding
305 homology (CAB), SERTA, PHD-Bromo binding (PBB), and C-terminal (Hirai et al.). To
306 identify the domains essential for circadian regulation, we utilized the CRISPR/Cas9 technique
307 to generate mutants in which the conserved domains were removed from the *tara* genomic locus
308 (Fig. 4A). Deletion of the SERTA domain led to lethality. In contrast, flies in which the CAB,
309 PBB, or CT domain was deleted were viable. We assayed SERTA deletion mutants in trans to
310 the hypomorphic $tara^{s132}$ allele and homozygous mutants for all other deletions for circadian
311 locomotor behavior. Compared with s132/+ heterozygous flies, the s132/ΔSERTA trans-
312 heterozygous mutants exhibited a substantial reduction in rhythm strength, but their circadian
313 period was not significantly altered (Table 2, Fig. 4 B-D). However, given that the s132 allele is
314 hypomorphic, and s132/ΔSERTA trans-heterozygotes retain some wild-type TARA protein, we
315 cannot rule out the possibility that the SERTA domain plays a role in determining the period
316 length. The lack of period change in s132/ΔSERTA mutants could be because the more strongly

317 affected mutants were arrhythmic and therefore excluded from the period analysis. Homozygous
318 CAB, PBB, or CT domain deletions had little effect on the period length (Table 2, Fig. 4B,C),
319 but they significantly reduced the strength of the locomotor rhythms (Table 2, Fig. 4B,D),
320 suggesting that they also contribute to rhythmic locomotor behavior. Our results indicate that all
321 four conserved domains play a role in maintaining rhythm strength.
322
323 **TARA interacts with VRI and PDP1 to modulate *Clk* transcription**
324 Considering the role mammalian homologs of TARA play in transcriptional coregulation
325 (Hsu et al., 2001), our discovery that TARA modulates the period length suggests that TARA
326 acts as a transcriptional coregulator of core clock components. We hypothesized that TARA
327 influences VRI activity, since *tara* and *vri* mutants exhibit similar circadian phenotypes.
328 Overexpression of *tara* or *vri* in PDF-expressing neurons leads to lengthened period (Table 1,
329 Fig. 3 C-E; Blau and Young, 1999), and both *tara* and *vri* mutants have decreased PDF
330 expression in s-LN_vs dorsal projections (Fig. 2C,D; Gunawardhana and Hardin, 2017).
331 Consequently, we investigated whether TARA regulates *Clk* transcription repression by VRI. For
332 this purpose, we employed *Drosophila* S2 cells transfected with a *Clk-luc* reporter that contains a
333 D-box element, a common binding site for PDP1 and VRI (Cyran et al., 2003). Previous work
334 has shown that VRI binds the same D-box element of the *Clk* promoter as PDP1, acting as a
335 competitive repressor (Cyran et al., 2003). Since repression by VRI would not be evident without
336 *Clk* transcription activation by PDP1, we co-transfected PDP1 and VRI at varying levels of
337 TARA.
338 A prior study used mammalian HEK293 cells to demonstrate PDP1-dependent *Clk*
339 transcription activation because it was not detectable in S2 cells (Cyran et al., 2003).

340 Intriguingly, we observed PDP1-dependent *Clk* transcription in *Drosophila* S2 cells when TARA
341 was co-transfected with PDP1 (Fig. 5A). Little PDP1 activity was observed without co-
342 transfected TARA, while PDP1 activity increased up to ~5-fold with rising TARA levels.
343 Transfection of TARA alone did not influence *Clk* transcription (Fig. 5A), in line with its lack of
344 a DNA binding domain and its function as a transcriptional coregulator rather than a
345 transcription factor. VRI co-transfection repressed PDP1-dependent *Clk* transcription, verifying
346 VRI's role as a competitive repressor of PDP1 (Fig. 5A). The degree of VRI-mediated
347 suppression of *Clk* transcription intensified with increasing levels of TARA. Intermediate TARA
348 levels, which significantly affected PDP1 activity, had little to moderate impact on VRI activity,
349 but higher TARA levels resulted in robust suppression of PDP1 activity by VRI (Fig. 5A).
350 However, since VRI suppressed nearly all PDP1-mediated *Clk* transcription at every level of
351 TARA, the smaller VRI-dependent suppression at lower levels of TARA may be attributed to
352 lower PDP1 activity rather than lower VRI activity.
353 To investigate the impact of TARA on VRI activity directly without co-transfected
354 PDP1, we utilized VRI fused to the viral VP16 transactivation domain (VRI::VP16), which
355 converts the repressor into a transcriptional activator (Cyran et al., 2003). We were unable to
356 express detectable amounts of VRI::VP16 in *Drosophila* S2 cells, possibly due to lethality
357 caused by its expression. Therefore, we turned to HEK293 cells, as a previous study
358 demonstrated *Clk* transcription by VRI::VP16 using the cell line (Cyran et al., 2003). Consistent
359 with the previous finding, VRI::VP16 promoted *Clk* transcription without co-transfected TARA
360 (Fig. 5B). Importantly, we discovered that co-transfected TARA upregulated VRI::VP16-
361 dependent *Clk* transcription up to ~4 fold in a dose-dependent manner, demonstrating TARA's
362 role in enhancing VRI activity. Moreover, TRIP-Br1 and TRIP-Br2, two mammalian homologs

363 of TARA, exhibited a moderate effect on VRI::VP16-dependent *Clk* transcription as well,
364 suggesting a conserved mechanism (Fig. 5B).
365 To evaluate whether TARA impacts *Clk* transcription by influencing PDP1 and VRI
366 protein levels, we conducted a Western analysis using cell lysates following transfection in S2
367 cells. Since transcriptional activity occurs in the nucleus, we examined nuclear fractions. Co-
368 transfected TARA did not influence PDP1 or VRI levels (Fig. 5C-G), suggesting that TARA
369 enhances the transcriptional activity of PDP1 and VRI, not their expression or protein stability.
370 Although co-transfected VRI increased TARA and PDP1 protein levels (Fig. 5C-G), these
371 effects would not account for the observed effects of TARA on *Clk* transcription. Our data
372 support TARA's function as a transcriptional coregulator of VRI and PDP1.
373 We then inquired whether the effects of TARA on VRI and PDP1 were mediated by
374 physical interaction. Co-immunoprecipitation (Co-IP) experiments in S2 cells demonstrated that
375 TARA can indeed form a physical complex with VRI or PDP1 (Fig. 5H). Collectively, our
376 results indicate that TARA can physically interact with VRI and PDP1 to enhance the
377 transcriptional suppression of *Clk* by VRI and its activation by PDP1.
378
379 **TARA exhibits little impact on CLK and PER activity**
380 Our findings indicate that TARA plays a role in the PDP1/VRI feedback loop of the
381 *Drosophila* molecular clock. To ascertain whether TARA also modulates the CLK-CYC/PER-
382 TIM feedback loop, we utilized a *per-luc* reporter in S2 cells and co-transfected CLK with
383 TARA. CLK-mediated transcription of *per* in S2 cells did not require co-transfected TARA, in
384 agreement with previous findings (Darlington et al., 1998), and was unaffected by increasing
385 TARA levels (Fig. 5I).

386 To investigate whether TARA regulates the suppression of CLK activity by PER, we co-
387 transfected CLK with varying levels of PER in S2 cells, with or without TARA. As previously
388 reported **(**Darlington et al., 1998**),** PER repressed CLK-dependent transcription of *per* in a dose-
389 dependent manner (Fig. 5J). Notably, the effect of TARA at each level of PER and the
390 interaction between the effects of TARA and PER were not significant, indicating that PER
391 suppression is independent of TARA (Fig. 5J). Together, our results reveal that TARA exerts
392 minimal impact on CLK's transcriptional activity and PER's repressive activity, demonstrating
393 the specificity in TARA's function as a transcriptional coregulator.
394
395 **The SERTA domain is essential for transcriptional coregulation**
396 To investigate the role of TARA's conserved domains in transcriptional regulation, we
397 generated deletion constructs for each domain: ΔCAB, ΔSERTA, ΔPBB, and ΔCT (Fig. 6A). We
398 transfected full-length or domain-deletion TARA along with *Clk-luc* and PDP1 in S2 cells and
399 conducted Luciferase assays. The results showed that TARA lacking the SERTA domain
400 (ΔSERTA) exerted a markedly diminished effect on PDP1 activity compared to full-length
401 TARA (Fig. 6B), indicating that the SERTA domain is critical for TARA to enhance PDP1's
402 transcriptional activity. Deletion of the other conserved domains had little effect on PDP1-
403 dependent *Clk* transcription. Next, we examined whether the SERTA domain is essential for
404 TARA's enhancement of VRI transcriptional activity using VRI::VP16 and HEK293 cells. We
405 discovered that the SERTA domain deletion eliminated TARA's influence on VRI::VP16
406 activity (Fig. 6C). To determine the expression levels of deletion constructs and their effects on
407 PDP1 expression, we performed a Western analysis. The results demonstrated that the deletion
408 constructs were expressed at levels similar to or slightly higher than the wild-type TARA (Figure

409 6D,E). Furthermore, PDP1 expression was not significantly affected by deletion constructs (Fig.
410 6D,F), indicating that the reduced *Clk* transcription upon ΔSERTA transfection is not due to
411 diminished PDP1 expression. Taken together, our findings demonstrate that the SERTA domain
412 of TARA is essential for enhancing PDP1 and VRI activity.
413
414 ***tara* genetically interacts with *vri* and *Pdp1* to modulate the molecular clock *in vivo***
415 Since we discovered that TARA enhanced the transcriptional activity of VRI and PDP1
416 in cultured cells, we examined whether *tara* interacts with *vri* and *Pdp1* to modulate the
417 molecular clock *in vivo*. We overexpressed *vri* or *Pdp1* in PDF+ clock neurons, with or without
418 *tara* co-overexpression. We observed a pronounced increase in period length when *vri* was
419 overexpressed in LN_vs (Table 3, Fig. 7), consistent with previous findings (Blau and Young,
420 1999). Although overexpressing *tara* alone also significantly increased period length, co-
421 overexpressing both *tara* and *vri* shortened the period compared to overexpressing *vri* alone
422 (Table 3, Fig. 7), indicating a genetic interaction between *tara* and *vri*. TARA may lengthen the
423 circadian period by enhancing VRI activity when VRI is present at normal levels. However,
424 when VRI levels are elevated, additional TARA may not further amplify VRI's period-
425 lengthening effect, but instead, it may shorten the period through its effect on PDP1.
426 We observed a minor (~0.3 h) increase in period length when *Pdp1* was overexpressed
427 (Table 3, Fig. 7). This outcome may seem unexpected, given PDP1's role as a positive activator
428 of *Clk* transcription. However, the small effect is comparable to the previously reported ~0.2 h,
429 non-significant increase in the period length of *Pdp1*-overexpressing flies (Zheng et al., 2009).
430 Although overexpressing *tara* in PDF+ neurons led to a significantly longer period, co-

431 overexpression with *Pdp1* eliminated TARA's impact on the period length (Table 3, Fig. 7),
432 demonstrating that *tara* and *Pdp1* genetically interact to regulate the pace of the molecular clock.
433 Overexpression of *tara* alone had a small but significant effect on the robustness of
434 circadian rhythms, while overexpression of *vri* alone or in combination with *tara* had little effect
435 (Table 3, Fig. 7). Overexpression of *Pdp1* significantly weakened the strength of locomotor
436 rhythms, consistent with previous findings (Benito et al., 2007; Zheng et al., 2009). Co-
437 overexpression of *tara* and *Pdp1* further decreased the rhythm strength, but the decrease was not
438 statistically significant.
439 The effect of *tara* overexpression on the circadian period may appear more similar to that
440 of *vri* overexpression than *Pdp1* overexpression, as both *tara* and *vri* overexpression markedly
441 lengthen the period while *Pdp1* overexpression has only a minor effect. However, it is important
442 to note that this observation does not necessarily indicate that TARA has a greater impact on the
443 transcriptional activity of VRI compared to PDP1. Considering that TARA enhanced VRI and
444 PDP1 activity in S2 cells, the impact of *tara* overexpression on locomotor rhythms *in vivo* may
445 reflect the combined effects of enhancing both VRI and PDP1 activity. Indeed, when we co-
446 overexpressed *vri* and *Pdp1* in PDF+ clock neurons, we observed an increase in period length
447 similar to that of *tara* overexpression (Table 3, Fig. 7). Co-overexpressing *vri* and *Pdp1* also
448 resulted in a rhythm strength comparable to that of overexpressing *tara*. Collectively, our
449 findings indicate that *tara* interacts with *vri* and *Pdp1* to modulate the circadian period and
450 rhythm strength in *Drosophila*.

451 **Discussion**

452 The present study identifies TARA as a novel regulatory component of the interlocked
453 transcription-translation feedback loops in the *Drosophila* molecular clock. Whereas the primary
454 feedback loop involving CLK-CYC and PER-TIM in the *Drosophila* circadian clock has been
455 studied extensively (reviewed in Allada and Chung, 2010; Hardin, 2011; Tataroglu and Emery,
456 2015; Patke et al., 2020), the secondary loop, including VRI and PDP1, is relatively understudied
457 (Blau and Young, 1999; Cyran et al., 2003; Glossop et al., 2003; Benito et al., 2007; Zheng et al.,
458 2009; Ling et al., 2012; Gunawardhana and Hardin, 2017; Gunawardhana et al., 2021). Our
459 transcriptional assays reveal that TARA enhances the activity of both the negative and positive
460 arms of the secondary feedback loop. TARA has little effect on PER and CLK activity,
461 suggesting that TARA plays a more critical role in the secondary loop than the primary loop.
462 Consistent with the transcriptional assay results, our behavioral data demonstrate that *tara*
463 genetically interacts with *vri* and *Pdp1* to regulate the pace of the *Drosophila* circadian clock.
464 *tara* mutants display markedly impaired locomotor rhythmicity despite robust PER cycling,
465 suggesting that TARA plays an additional role in the circadian output pathway. These findings
466 are reminiscent of previous results showing that VRI and PDP1 play critical roles in the
467 molecular clock and the circadian output pathway (Blau and Young, 1999; Cyran et al., 2003;
468 Glossop et al., 2003; Benito et al., 2007; Zheng et al., 2009; Ling et al., 2012; Gunawardhana
469 and Hardin, 2017; Gunawardhana et al., 2021), supporting the view that TARA functions with
470 VRI and PDP1 to regulate circadian rhythms. We previously reported that TARA promotes sleep
471 through its interaction with CycA and Cdk1 in a subset of neurons in the *pars lateralis*, a region
472 considered analogous to the mammalian hypothalamus (Afonso et al., 2015b). Collectively, these

473 findings suggest that TARA regulates circadian rhythms and sleep by interacting with different
474 molecular partners in distinct neuronal populations.

475 Given that TARA enhances both the activator and suppressor of *Clk* transcription, *tara*
476 overexpression might be expected to have little effect on the circadian period. However, *vri*
477 overexpression leads to a markedly long period, while *Pdp1*overexpression has a slight period-
478 lengthening effect. Therefore, the combined effect of enhancing both VRI and PDP1 is expected
479 to be a longer period compared to control flies. Indeed, we find that *tara* overexpression
480 lengthens the circadian period, mirroring the consequence of simultaneously overexpressing *vri*
481 and *Pdp1*. It is unclear why *vri* overexpression affects the clock speed more than *Pdp1*
482 overexpression. A previous study demonstrated that VRI expression peaks a few hours before
483 PDP1 through an as-yet unidentified mechanism (Cyran et al., 2003). The earlier accumulation
484 of VRI may be linked to a more potent effect of *vri* overexpression on the circadian period.
485 Considering that PDP1 is an activator of *Clk* transcription and *Clk* overexpression shortens the
486 circadian period (Zhao et al., 2003), it is unclear why *Pdp1* overexpression leads to a slightly
487 lengthened period. PDP1 likely has multiple target genes, and the combined effects of PDP1
488 overexpression on *Clk* and other target genes may be a small increase in the circadian period.

489 The components of the primary feedback loop in the molecular clock are highly
490 conserved between flies and mammals (reviewed in Allada and Chung, 2010; Hardin, 2011;
491 Tataroglu and Emery, 2015; Patke et al., 2020). Mammalian CLK, BMAL1 (a CYC homolog),
492 and PER1/2/3 perform similar functions as their *Drosophila* orthologs, while
493 CRYPTOCHROME (CRY)1/2 are functionally equivalent to *Drosophila* TIM. However, the
494 functions of the secondary feedback loop involving VRI and PDP1 in *Drosophila* are performed
495 by more complex, multi-layered feedback loops in mammals. The layered loops include nuclear

496 receptors, REV-ERBα/β (also known as NR1D1/2), and Retinoid-related Orphan Receptor
497 (ROR)α/β/δ, which competitively bind the RRE element in the promotor of RRE-containing
498 genes, including *BMAL1*, to activate and suppress its transcription (Preitner et al., 2002; Ueda et
499 al., 2002; Sato et al., 2004). REV-ERBs and RORs are not homologs of VRI and PDP1, but
500 mammalian homologs of VRI and PDP1, named Nuclear Factor Interleukin-3-Regulated Protein
501 (NFIL3, also known as E4BP4) and D-BOX BINDING PROTEIN (DBP), respectively, also
502 participate in the interlocked feedback loops. Like their *Drosophila* homologs, NFIL3 and DBP
503 competitively bind the D-box element to inhibit and activate the transcription of D-box-
504 containing genes, including RORs (Mitsui et al., 2001). RORs activate *NFIL3* transcription,
505 while NFIL3 inhibits the transcription of *ROR*s, forming a feedback loop (Mitsui et al., 2001;
506 Gachon et al., 2004; Ueda et al., 2005). Taken together, REV-ERBs and NFIL3 suppress *BMAL1*
507 transcription, while RORs and DBP activate *BMAL1* transcription. These findings suggest that
508 VRI performs the combined functions of REV-ERBs and NFIL3, while PDP1 performs the
509 combined functions of RORs and DBP. Initial studies demonstrating that VRI and PDP1 regulate
510 *Clk* transcription were performed in mammalian HEK293 cells because PDP1 did not activate
511 *Clk* transcription in S2 cells (Cyran et al., 2003). Our data show that TARA is the missing factor
512 necessary for *Clk* transcription by PDP1 in *Drosophila* S2 cells. HEK293 cells may express
513 sufficient levels of TRIP-Br proteins, the mammalian homologs of TARA, to allow PDP1
514 activity at the *Clk* promoter. These considerations and our finding that TRIP-Br1/2 enhance VRI
515 activity in HEK293 cells raise the intriguing possibility that TRIP-Br proteins regulate the
516 mammalian circadian period through their interactions with NFIL3 and DBP for the transcription
517 of D-box-containing genes.

518 TARA and TRIP-Br proteins contain four conserved domains. The function of the
519 SERTA domain is not well understood (Calgaro et al., 2002; Manansala et al., 2013). The
520 present study uncovers a novel role of the SERTA domain in enhancing PDP1 and VRI activity
521 and regulating the pace of the *Drosophila* circadian clock. We also find that TARA is a critical
522 regulator of rhythm amplitude and that all four domains contribute to robust locomotor rhythms.
523 It would be interesting to investigate further the molecular functions of the conserved domains
524 and their role in circadian rhythms.

525 TARA is ubiquitously expressed in neurons (Afonso et al., 2015b), but what regulates
526 TARA expression or activity is largely unknown. Notably, chromatin immunoprecipitation tiling
527 array assays (Abruzzi et al., 2011) detected cyclic CLK binding to a promoter region of *tara*,
528 suggesting that it is a direct transcriptional target of CLK. Although we did not observe daily
529 cycling of TARA protein levels in s-LN_vs (Afonso et al., 2015a), TARA activity may exhibit
530 circadian cycling, since its partners VRI and PDP1 undergo circadian cycling. TARA levels or
531 activity may also respond to changing environmental and internal conditions, such as the
532 metabolic state. Earlier findings suggest that mammalian homologs of TARA are involved in
533 metabolic regulation. TRIP-Br2 is involved in lipid and oxidative metabolism in adult mice
534 (Liew et al., 2013), and prolonged nutrient starvation dramatically decreases TRIP-Br3 to induce
535 apoptosis (Li et al., 2015). Circadian regulation is closely linked to metabolism (Bailey et al.,
536 2014; Asher and Sassone-Corsi, 2015; Guan and Lazar, 2021), and TARA may play a role in
537 integrating circadian and metabolic regulation. Further studies will need to be performed to
538 examine the potential role of TARA in linking circadian rhythms and metabolism.

539 Our findings reveal a novel role for *tara* in regulating the pace of the circadian clock
540 through its interaction with *vri* and *Pdp1* in the secondary feedback loop of the *Drosophila*

541 circadian clock. They provide a rationale for investigating the role of the TRIP-Br proteins in
542 regulating circadian rhythms and their potential interaction with NFIL3 and DBP in the
543 mammalian molecular clock.

544 **References**

545 Abruzzi KC, Rodriguez J, Menet JS, Desrochers J, Zadina A, Luo W, Tkachev S, Rosbash M
546 (2011) Drosophila CLOCK target gene characterization: implications for circadian tissue-
547 specific gene expression. Genes Dev 25:2374-2386.

548 Afonso DJ, Machado DR, Koh K (2015a) Control of sleep by a network of cell cycle genes. Fly
549 (Austin) 9:165-172.

550 Afonso DJ, Liu D, Machado DR, Pan H, Jepson JE, Rogulja D, Koh K (2015b) TARANIS
551 Functions with Cyclin A and Cdk1 in a Novel Arousal Center to Control Sleep in
552 Drosophila. Curr Biol 25:1717-1726.

553 Allada R, Chung BY (2010) Circadian organization of behavior and physiology in Drosophila.
554 Annu Rev Physiol 72:605-624.

555 Allada R, White NE, So WV, Hall JC, Rosbash M (1998) A mutant Drosophila homolog of
556 mammalian Clock disrupts circadian rhythms and transcription of period and timeless.
557 Cell 93:791-804.

558 Asher G, Sassone-Corsi P (2015) Time for food: the intimate interplay between nutrition,
559 metabolism, and the circadian clock. Cell 161:84-92.

560 Bailey SM, Udoh US, Young ME (2014) Circadian regulation of metabolism. J Endocrinol
561 222:R75-96.

562 Benito J, Zheng H, Hardin PE (2007) PDP1epsilon functions downstream of the circadian
563 oscillator to mediate behavioral rhythms. J Neurosci 27:2539-2547.

564 Blau J, Young MW (1999) Cycling vrille expression is required for a functional Drosophila
565 clock. Cell 99:661-671.

566 Brand AH, Perrimon N (1993) Targeted gene expression as a means of altering cell fates and
567 generating dominant phenotypes. Development 118:401-415.
568 Calgaro S, Boube M, Cribbs DL, Bourbon HM (2002) The Drosophila gene taranis encodes a
569 novel trithorax group member potentially linked to the cell cycle regulatory apparatus.
570 Genetics 160:547-560.
571 Cyran SA, Buchsbaum AM, Reddy KL, Lin MC, Glossop NR, Hardin PE, Young MW, Storti
572 RV, Blau J (2003) vrille, Pdp1, and dClock form a second feedback loop in the
573 Drosophila circadian clock. Cell 112:329-341.
574 Darlington TK, Wager-Smith K, Ceriani MF, Staknis D, Gekakis N, Steeves TD, Weitz CJ,
575 Takahashi JS, Kay SA (1998) Closing the circadian loop: CLOCK-induced transcription
576 of its own inhibitors per and tim. Science 280:1599-1603.
577 Dutta P, Li WX (2017) The SERTAD protein Taranis plays a role in Polycomb-mediated gene
578 repression. PLoS One 12:e0180026.
579 Gachon F, Fonjallaz P, Damiola F, Gos P, Kodama T, Zakany J, Duboule D, Petit B, Tafti M,
580 Schibler U (2004) The loss of circadian PAR bZip transcription factors results in
581 epilepsy. Genes Dev 18:1397-1412.
582 George H, Terracol R (1997) The vrille gene of Drosophila is a maternal enhancer of
583 decapentaplegic and encodes a new member of the bZIP family of transcription factors.
584 Genetics 146:1345-1363.
585 Glossop NR, Houl JH, Zheng H, Ng FS, Dudek SM, Hardin PE (2003) VRILLE feeds back to
586 control circadian transcription of Clock in the Drosophila circadian oscillator. Neuron
587 37:249-261.

588 Guan D, Lazar MA (2021) Interconnections between circadian clocks and metabolism. J Clin
589 Invest 131.
590 Gunawardhana KL, Hardin PE (2017) VRILLE Controls PDF Neuropeptide Accumulation and
591 Arborization Rhythms in Small Ventrolateral Neurons to Drive Rhythmic Behavior in
592 Drosophila. Curr Biol 27:3442-3453 e3444.
593 Gunawardhana KL, Rivas GBS, Caster C, Hardin PE (2021) Crosstalk between vrille transcripts,
594 proteins, and regulatory elements controlling circadian rhythms and development in
595 Drosophila. iScience 24:101893.
596 Hardin PE (2011) Molecular genetic analysis of circadian timekeeping in Drosophila. Adv Genet
597 74:141-173.
598 Hardin PE, Hall JC, Rosbash M (1990) Feedback of the Drosophila period gene product on
599 circadian cycling of its messenger RNA levels. Nature 343:536-540.
600 Hirai T, Ramos TL, Lin P-Y, Simonetta F, Su LL, Picton LK, Baker J, Lin J-X, Li P, Seo K,
601 Lohmeyer JK, Bolivar-Wagers S, Mavers M, Leonard WJ, Blazar BR, Garcia KC, Negrin
602 RS (2021) Selective expansion of regulatory T cells using an orthogonal IL-2/IL-2
603 receptor system facilitates transplantation tolerance. The Journal of clinical investigation
604 131.
605 Hsu SI, Yang CM, Sim KG, Hentschel DM, O'Leary E, Bonventre JV (2001) TRIP-Br: a novel
606 family of PHD zinc finger- and bromodomain-interacting proteins that regulate the
607 transcriptional activity of E2F-1/DP-1. EMBO J 20:2273-2285.
608 Li C, Jung S, Lee S, Jeong D, Yang Y, Kim KI, Lim JS, Cheon CI, Kim C, Kang YS, Lee MS
609 (2015) Nutrient/serum starvation derived TRIP-Br3 down-regulation accelerates
610 apoptosis by destabilizing XIAP. Oncotarget 6:7522-7535.

611 Liew CW, Boucher J, Cheong JK, Vernochet C, Koh HJ, Mallol C, Townsend K, Langin D,
612 Kawamori D, Hu J, Tseng YH, Hellerstein MK, Farmer SR, Goodyear L, Doria A,
613 Bluher M, Hsu SI, Kulkarni RN (2013) Ablation of TRIP-Br2, a regulator of fat lipolysis,
614 thermogenesis and oxidative metabolism, prevents diet-induced obesity and insulin
615 resistance. Nat Med 19:217-226.
616 Ling J, Dubruille R, Emery P (2012) KAYAK-alpha modulates circadian transcriptional
617 feedback loops in Drosophila pacemaker neurons. J Neurosci 32:16959-16970.
618 Manansala MC, Min S, Cleary MD (2013) The Drosophila SERTAD protein Taranis determines
619 lineage-specific neural progenitor proliferation patterns. Dev Biol 376:150-162.
620 Mitsui S, Yamaguchi S, Matsuo T, Ishida Y, Okamura H (2001) Antagonistic role of E4BP4 and
621 PAR proteins in the circadian oscillatory mechanism. Genes Dev 15:995-1006.
622 Partch CL, Green CB, Takahashi JS (2014) Molecular architecture of the mammalian circadian
623 clock. Trends Cell Biol 24:90-99.
624 Patke A, Young MW, Axelrod S (2020) Molecular mechanisms and physiological importance of
625 circadian rhythms. Nat Rev Mol Cell Biol 21:67-84.
626 Preitner N, Damiola F, Lopez-Molina L, Zakany J, Duboule D, Albrecht U, Schibler U (2002)
627 The orphan nuclear receptor REV-ERBalpha controls circadian transcription within the
628 positive limb of the mammalian circadian oscillator. Cell 110:251-260.
629 Reddy KL, Wohlwill A, Dzitoeva S, Lin MH, Holbrook S, Storti RV (2000) The Drosophila
630 PAR domain protein 1 (Pdp1) gene encodes multiple differentially expressed mRNAs
631 and proteins through the use of multiple enhancers and promoters. Dev Biol 224:401-414.

632 Renn SC, Park JH, Rosbash M, Hall JC, Taghert PH (1999) A pdf neuropeptide gene mutation
633 and ablation of PDF neurons each cause severe abnormalities of behavioral circadian
634 rhythms in Drosophila. Cell 99:791-802.
635 Sato TK, Panda S, Miraglia LJ, Reyes TM, Rudic RD, McNamara P, Naik KA, FitzGerald GA,
636 Kay SA, Hogenesch JB (2004) A functional genomics strategy reveals Rora as a
637 component of the mammalian circadian clock. Neuron 43:527-537.
638 Takahashi JS (2017) Transcriptional architecture of the mammalian circadian clock. Nat Rev
639 Genet 18:164-179.
640 Tataroglu O, Emery P (2015) The molecular ticks of the Drosophila circadian clock. Curr Opin
641 Insect Sci 7:51-57.
642 Ueda HR, Hayashi S, Chen W, Sano M, Machida M, Shigeyoshi Y, Iino M, Hashimoto S (2005)
643 System-level identification of transcriptional circuits underlying mammalian circadian
644 clocks. Nat Genet 37:187-192.
645 Ueda HR, Chen W, Adachi A, Wakamatsu H, Hayashi S, Takasugi T, Nagano M, Nakahama K,
646 Suzuki Y, Sugano S, Iino M, Shigeyoshi Y, Hashimoto S (2002) A transcription factor
647 response element for gene expression during circadian night. Nature 418:534-539.
648 Wu MN, Joiner WJ, Dean T, Yue Z, Smith CJ, Chen D, Hoshi T, Sehgal A, Koh K (2010)
649 SLEEPLESS, a Ly-6/neurotoxin family member, regulates the levels, localization and
650 activity of Shaker. Nat Neurosci 13:69-75.
651 Zhao J, Kilman VL, Keegan KP, Peng Y, Emery P, Rosbash M, Allada R (2003) Drosophila
652 clock can generate ectopic circadian clocks. Cell 113:755-766.
653 Zheng X, Sehgal A (2012) Speed control: cogs and gears that drive the circadian clock. Trends
654 Neurosci 35:574-585.

655 Zheng X, Koh K, Sowcik M, Smith CJ, Chen D, Wu MN, Sehgal A (2009) An isoform-specific
656 mutant reveals a role of PDP1 epsilon in the circadian oscillator. J Neurosci 29:10920-
657 10927.
658

659 **Figure Legends**

660

661 **Figure 1. Pan-neuronal and clock-neuron-specific knockdown of *tara* degrades rhythm**
662 **strength. (A)** Representative circadian actograms of females of the following genotypes in DD:
663 pan-neuronal knockdown (*elav* > *tara* RNAi), clock-neuron-specific knockdown (*tim* > *tara*
664 RNAi), LN_v-specific knockdown (*Pdf* > *tara* RNAi), and their respective *Gal4* driver controls
665 (*elav* > +, *tim* > +, and *Pdf* > +). In this figure and subsequent figures, the gray and black bars
666 above the actogram indicate subjective day and night, respectively. **(B)** Period length (top) and
667 rhythm strength (bottom) of females of indicated genotypes. N = 29-61 for period length; n = 29-
668 71 for rhythm strength. Red labels indicate female flies, while blue labels indicate male flies. The
669 horizontal dotted line represents the mean period length (top) and rhythm strength (bottom) of
670 the common control (+ > *tara* RNAi). **(C)** Representative circadian actograms of males of
671 indicated genotypes in DD. **(D)** Period length (top) and rhythm strength (bottom) of males of
672 indicated genotypes. N = 31-47 for period length and rhythm strength. Mean ± SEM is shown.
673 ****$p < 0.0001$, ns: not significant; Brown-Forsythe and Welch ANOVA tests followed by
674 Dunnett's T3 multiple comparisons test relative to both parental controls (B and D).

675

676 **Figure 2. PER cycling and PDF accumulation are altered in the s-LN_v of *tara* mutants. (A)**
677 Representative expression patterns of PER and PDF in the s-LN_vs of control and $tara^{s132/1}$ males
678 at the indicated circadian times on the 3rd day in DD. The scale bar is 10 μm. **(B)** Quantification
679 of PER levels in s-LN_vs for control and $tara^{s132/1}$ males (n = 11-19). **(C)** Representative PDF
680 expression patterns in the dorsal projections of s-LN_vs at the indicated circadian times on the 3rd
681 day in DD in control and $tara^{s132/1}$ males. Signal intensity is indicated using the "royal" lookup

682 table, where black represents the minimum intensity, and white represents the maximum
683 intensity. The scale bar is 20 μm. **(D)** Quantification of PDF levels in the dorsal projection of s-
684 LN_vs for control and *tara*$^{s132/1}$ males (n = 15-18). **(E)** Quantification of *Pdf* mRNA levels from
685 whole head extracts for control and *tara*$^{s132/1}$ males. Six independent biological samples, each
686 from 30 fly heads, were assayed. Mean ± SEM is shown. ****$p < 0.0001$, ***$p < 0.001$, **$p <$
687 0.01, *$p < 0.05$, ns: not significant; two-way ANOVA followed by Sidak's multiple comparisons
688 tests (B and D); Welch's *t*-test (E).
689
690 **Figure 3. Overexpression of TARA in LN_vs results in slower PER cycling and lengthened**
691 **circadian period. (A)** Representative expression patterns of PER and PDF in s-LN_vs of flies
692 overexpressing TARA (*Pdf* > *tara*) and parental controls at the indicated circadian times on the
693 3rd day in DD. The scale bar is 10 μm. **(B)** PER signal quantification in s-LN_vs (n = 8-16). **(C)**
694 Representative circadian actograms of male flies overexpressing *tara* in PDF-positive LN_vs (*Pdf*
695 > *tara*) and their parental controls. **(D-E)** Period length (D) and rhythm strength (E) of males of
696 indicated genotypes. Mean ± SEM is shown. ****$p < 0.0001$, ns: not significant; two-way
697 ANOVA followed by Tukey's post hoc test (B); Brown-Forsythe and Welch ANOVA tests
698 followed by Dunnett's T3 multiple comparisons tests (D and E).
699
700 **Figure 4. Deletion of conserved TARA domains significantly reduces rhythm strength. (A)**
701 Amino acid sequences of conserved TARA domains (boxed) and their flanking sequences. The
702 numbers indicate the positions in the TARA-B sequence. Conserved amino acids are shown in
703 bold. The dashes represent deleted amino acids, and gray indicates substituted amino acids. (**B)**
704 Representative circadian actograms of indicated genotypes. (**C-D)** Period length (C) and rhythm

705 strength (D) of males of indicated genotypes. Mean ± SEM is shown. ****p<0.0001, **p<0.001,
706 ns: not significant; one-way Brown-Forsythe and Welch ANOVA tests followed by Dunnett's T3
707 multiple comparisons test (C and D).
708
709 **Figure 5. TARA interacts with PDP1 and VRI to regulate *Clk* transcription**
710 **(A)** Luciferase activity of the *Clk-luc* reporter in *Drosophila* S2 cells transfected with UAS-*Pdp1*
711 (10 ng), UAS-*vri* (35 ng), and UAS-HA::*tara* (5 ng, 10 ng, or 15 ng) as indicated. Luciferase
712 activity was normalized to the condition that includes UAS-*Pdp1* and 15 ng of UAS-HA::*tara*
713 (+++). **(B)** Luciferase activity of the *Clk-luc* reporter in HEK293 cells transfected with CMV-
714 *vri::VP16* (5 ng), CMV-*tara* (10 ng or 30 ng), and CMV-*TRIP-Br1* or CMV-*TRIP-Br2* (30 ng)
715 as indicated. Relative luciferase activity compared to the condition in which CMV-*vri::VP16*
716 alone is transfected is presented. **(C-D).** Representative Western blot of *Drosophila* S2 cells
717 transfected with the *Clk-luc* reporter, UAS-*Pdp1*, UAS-*vri*, and UAS-HA::*tara*, as indicated.
718 Antibodies against HA, PDP1, VRI, and Histone H3 were used. (**E-G)** Quantification of TARA
719 (E), PDP1 (F), and VRI (G) expression levels. **(H)** TARA forms a physical complex with VRI
720 and PDP1 in S2 cells. V5::TARA was immunoprecipitated with an anti-V5 antibody, and
721 antibodies against TARA, PDP1, and VRI were used for Western blotting. **(I)** Luciferase activity
722 of the *per-luc* reporter in *Drosophila* S2 cells transfected with UAS-HA::*tara* (10 ng or 30 ng),
723 and UAS-*Clk* (1 ng). Relative luciferase activity compared to the condition in which UAS-*Clk*
724 alone is transfected is presented. **(J)** The assay was conducted as in (I), except with three doses
725 of co-transfected UAS-*per* (2 ng, 5 ng, or 10 ng). Mean ± SEM is shown. ***p<0.001, **p<0.01,
726 *p<0.05, ns: not significant; two-way ANOVA followed by Tukey's post hoc tests (A); Welch's
727 *t*-test (E); one-way Brown-Forsythe and Welch ANOVA followed by Dunnett's T3 multiple

728 comparisons test (F-G, and I); two-way ANOVA followed by Sidak's multiple comparisons tests
729 (J). The effect of PER levels on *per-luc* activity was significant irrespective of the presence (+)
730 or absence (-) of TARA. None of the pairwise comparisons of the +TARA vs. -TARA conditions
731 at each level of PER revealed a significant difference (J).
732
733 **Figure 6. TARA enhances the transcriptional activity of PDP1 and VRI and forms a**
734 **physical complex with them. (A)** Schematic of TARA domain deletion mutants. **(B)** Luciferase
735 activity of the *Clk-luc* reporter in *Drosophila* S2 cells transfected with 30 ng of full-length UAS-
736 HA::*tara* (WT) or HA-tagged TARA domain deletion constructs (ΔCAB, ΔSERTA, ΔPBB, and
737 ΔCT). Luciferase activity compared to the condition in which UAS-*Pdp1* is transfected with full-
738 length TARA is presented. **(C)** Luciferase activity of the *Clk-luc* reporter in HEK293 cells
739 transfected with 5 ng of CMV-*vri::VP16* and 30 ng of full-length CMV-*tara* (WT) or a SERTA
740 domain deletion construct (ΔSERTA). Relative luciferase activity compared to the condition in
741 which CMV-*vri::VP16* is transfected with full-length CMV-*tara* is presented. **(D)** Western blot
742 of *Drosophila* S2 cells transfected with a *Clk-luc* reporter with 30 ng of full-length UAS-
743 HA::*tara* (WT) or HA-tagged domain deletion constructs (ΔCAB, ΔSERTA, ΔPBB, and ΔCT)
744 and 15 ng UAS-*Pdp1* as indicated. (**E-F**) Quantification of TARA (E) and PDP1 (F) expression
745 levels. Mean ± SEM is shown. ****$p<0.0001$, ***$p<0.001$, **$p<0.01$, *$p<0.05$, ns: not
746 significant; one-way Brown-Forsythe and Welch ANOVA followed by Dunnett's T3 multiple
747 comparisons test relative to a control condition (B,C,E, and F).
748
749 **Figure 7. *tara* regulates the clock speed through genetic interactions with *vri* and *Pdp1*.** (**A**)
750 Representative circadian actograms of males of indicated genotypes. (**B**) Period length (top) and

751 rhythm strength (bottom) of indicated genotypes. N = 36-64 for period length, n = 40-67 for

752 rhythm strength. The horizontal dotted line represents the mean period length (top) and rhythm

753 strength (bottom) for the common parental control (*Pdf* > +). Mean ± SEM is shown. ****p <

754 0.0001, ***p < 0.001, **p<0.01, *p < 0.05, ns: not significant; one-way Brown-Forsythe and

755 Welch ANOVA followed by Dunnett's T3 multiple comparisons test.

Figure 1

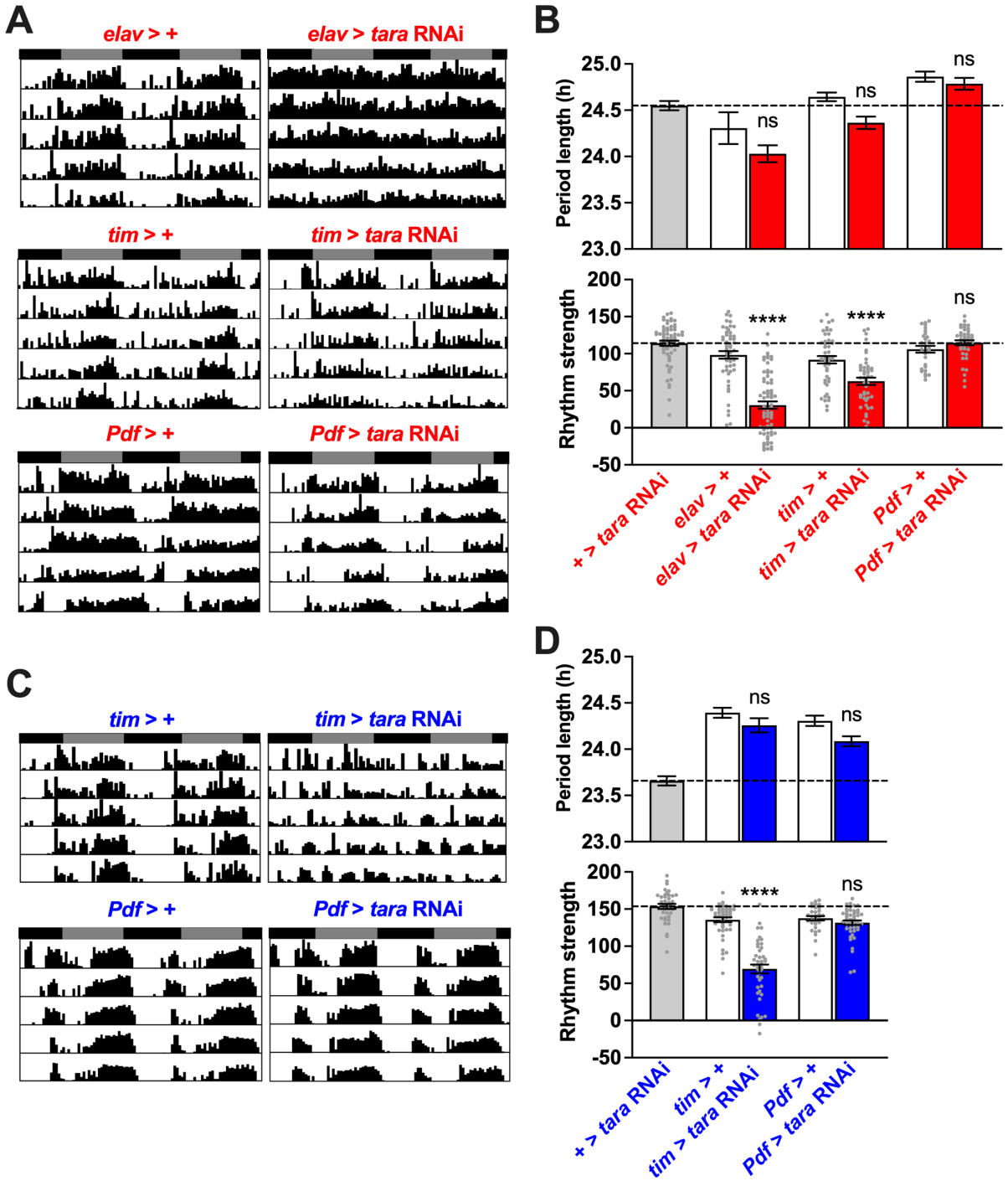
A
elav > +
elav > tara RNAi
tim > +
tim > tara RNAi
Pdf > +
Pdf > tara RNAi
B
Period length (h)
25.0
24.5
24.0
23.5
23.0
ns
ns
ns
Rhythm strength
200
150
100
50
0
-50
****
****
ns
+ > tara RNAi
elav > +
elav > tara RNAi
tim > +
tim > tara RNAi
Pdf > +
Pdf > tara RNAi
C
tim > +
tim > tara RNAi
Pdf > +
Pdf > tara RNAi
D
Period length (h)
25.0
24.5
24.0
23.5
23.0
ns
ns
Rhythm strength
200
150
100
50
0
-50
****
ns
+ > tara RNAi
tim > +
tim > tara RNAi
Pdf > +
Pdf > tara RNAi

756

Figure 2

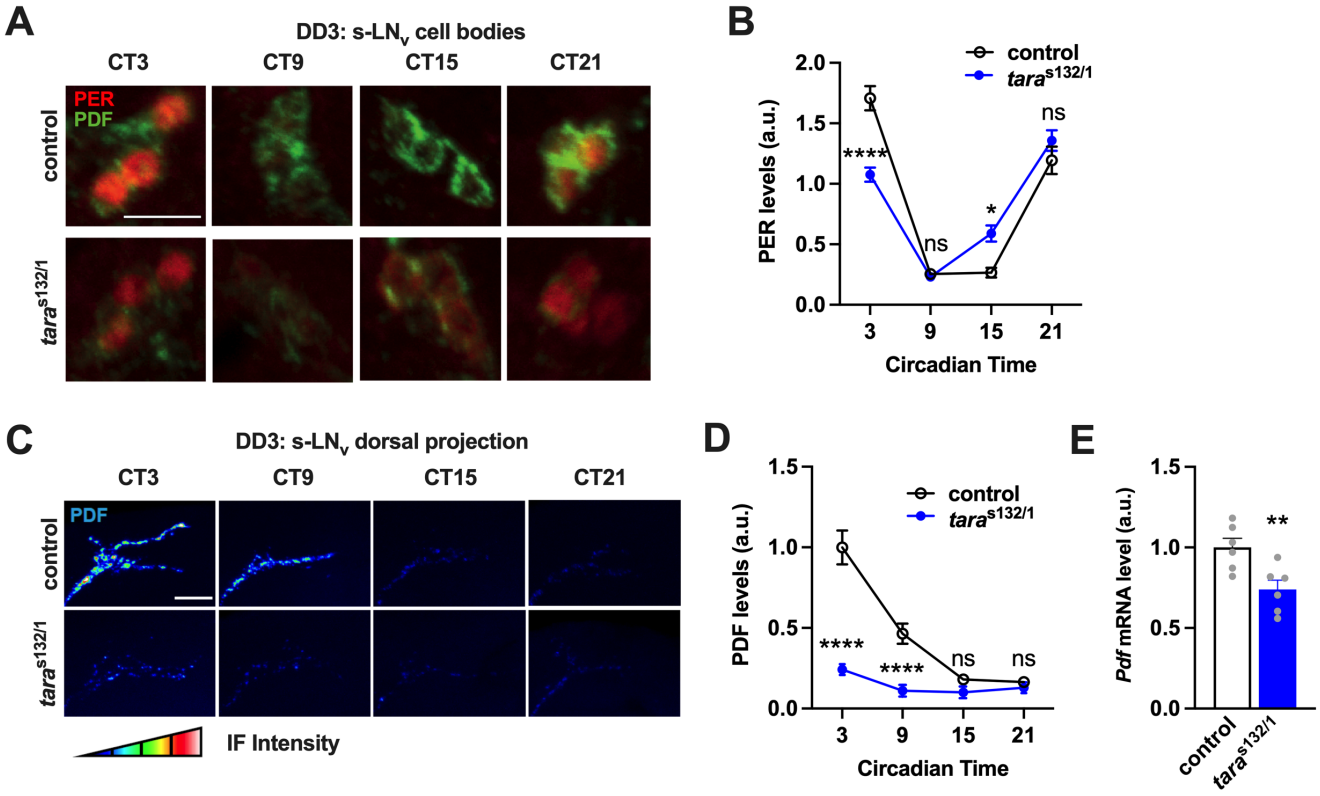
A
DD3: s-LNv cell bodies
CT3
CT9
CT15
CT21
PER
PDF
control
tara s132/1
B
control
tara s132/1
PER levels (a.u.)
2.0
1.5
1.0
0.5
0.0
****
ns
*
ns
3
9
15
21
Circadian Time
C
DD3: s-LNv dorsal projection
CT3
CT9
CT15
CT21
PDF
control
tara s132/1
IF Intensity
D
control
tara s132/1
PDF levels (a.u.)
1.5
1.0
0.5
0.0
****
****
ns
ns
3
9
15
21
Circadian Time
E
Pdf mRNA level (a.u.)
1.5
1.0
0.5
0.0
**
control
tara s132/1

757

Figure 3

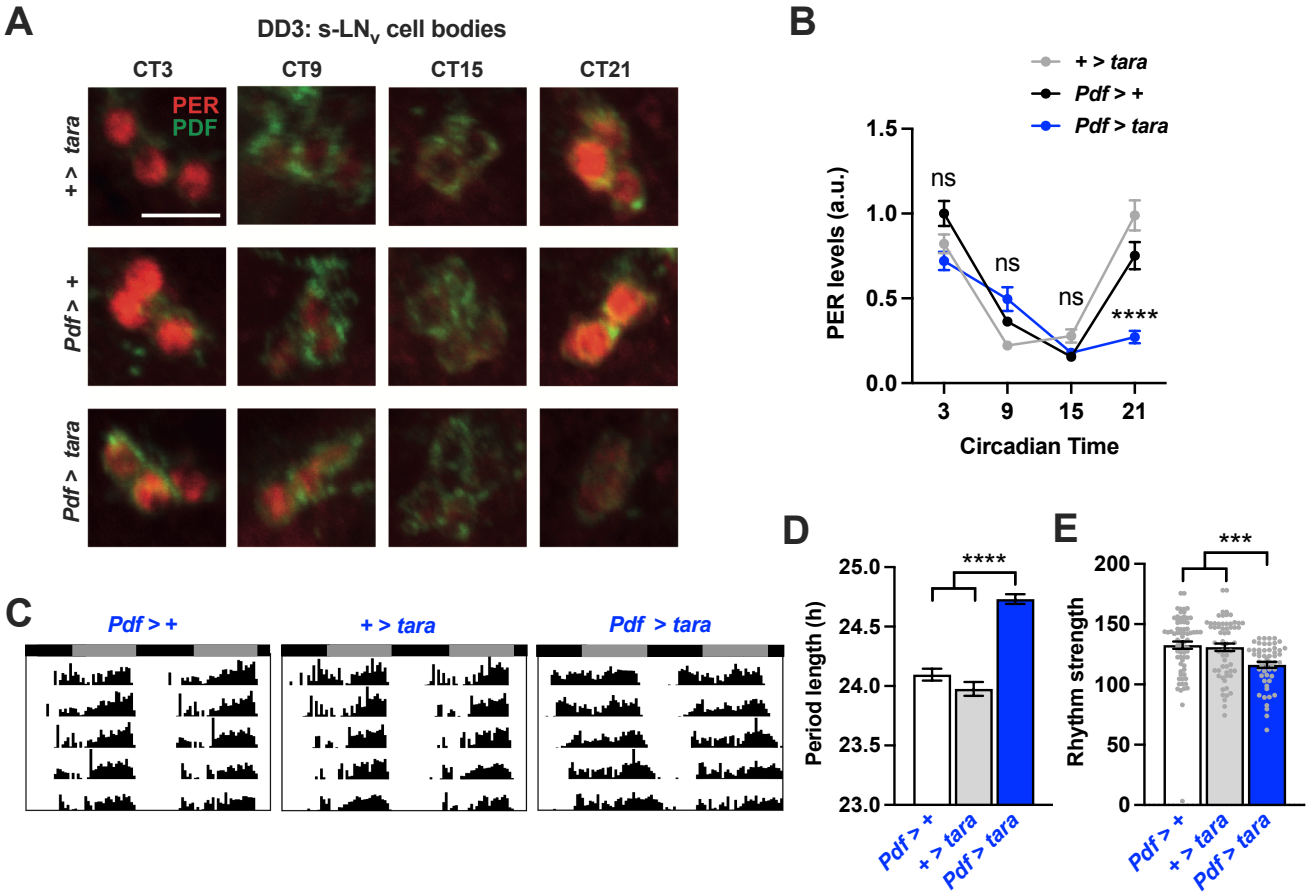
A
DD3: s-LNv cell bodies
CT3
CT9
CT15
CT21
PER
PDF
+ > tara
Pdf > +
Pdf > tara
B
+ > tara
Pdf > +
Pdf > tara
PER levels (a.u.)
1.5
1.0
0.5
0.0
ns
ns
ns
****
3
9
15
21
Circadian Time
C
Pdf > +
+ > tara
Pdf > tara
D
Period length (h)
25.0
24.5
24.0
23.5
23.0
****
Pdf > +
+ > tara
Pdf > tara
E
Rhythm strength
200
150
100
50
0
***
Pdf > +
+ > tara
Pdf > tara

758

Figure 4

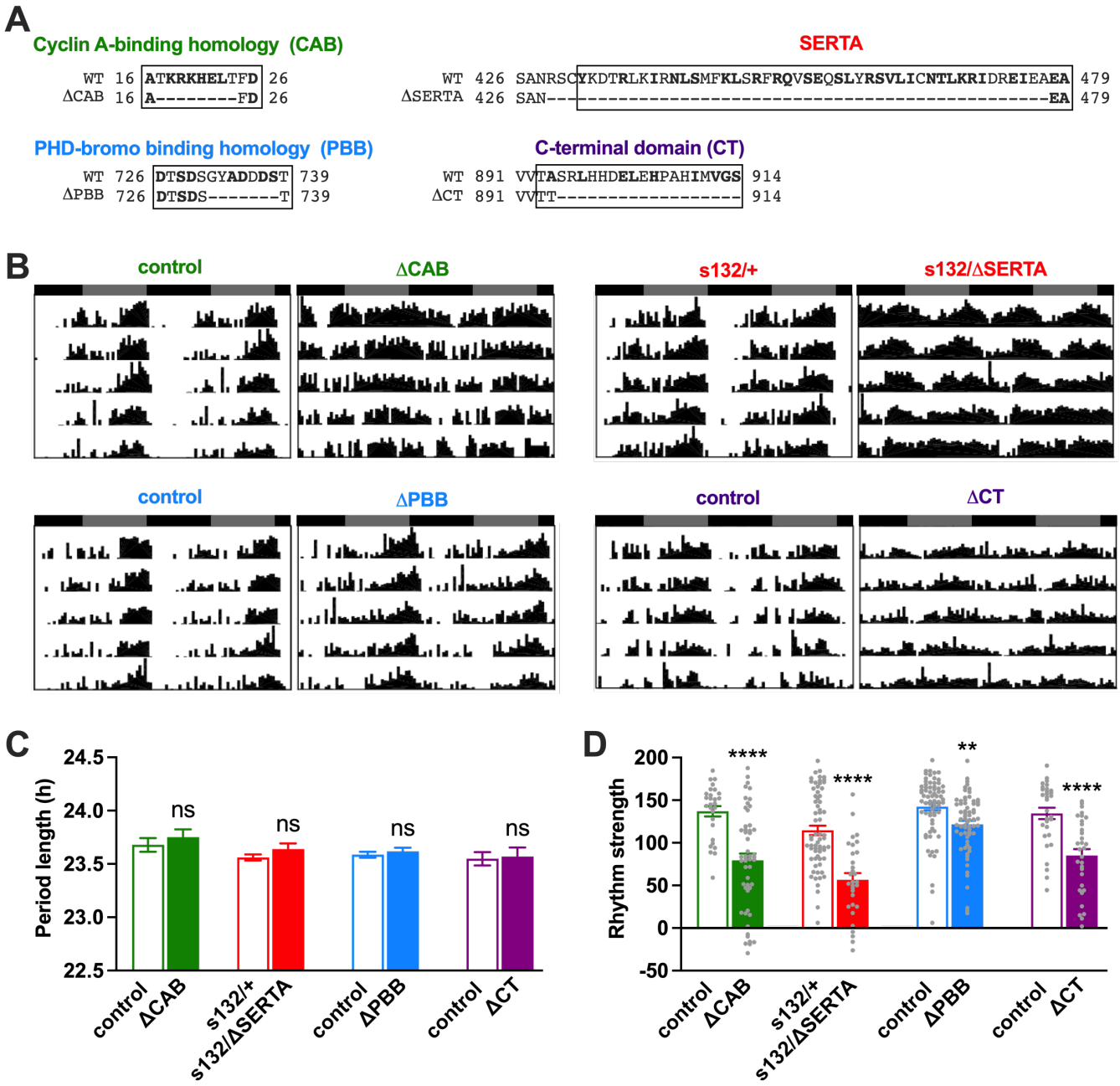
A
Cyclin A-binding homology (CAB)
WT 16 ATKRKHELTFD 26
ΔCAB 16 A--------FD 26
SERTA
WT 426 SANRSCYKDTRLKIRNLSMFKLSRFRQVSEQSLYRSVLICNTLKRIDREIEAEA 479
ΔSERTA 426 SAN----------EA 479
PHD-bromo binding homology (PBB)
WT 726 DTSDSGYADDDST 739
ΔPBB 726 DTSDS-------T 739
C-terminal domain (CT)
WT 891 VVTASRLHHDELEHPAHIMVGS 914
ΔCT 891 VVTT---------- 914
B
control
ΔCAB
s132/+
s132/ΔSERTA
control
ΔPBB
control
ΔCT
C
Period length (h)
24.5
24.0
23.5
23.0
22.5
ns
ns
ns
ns
control
ΔCAB
s132/+
s132/ΔSERTA
control
ΔPBB
control
ΔCT
D
Rhythm strength
200
150
100
50
0
-50
****
****
**
****
control
ΔCAB
s132/+
s132/ΔSERTA
control
ΔPBB
control
ΔCT

759

Figure 5

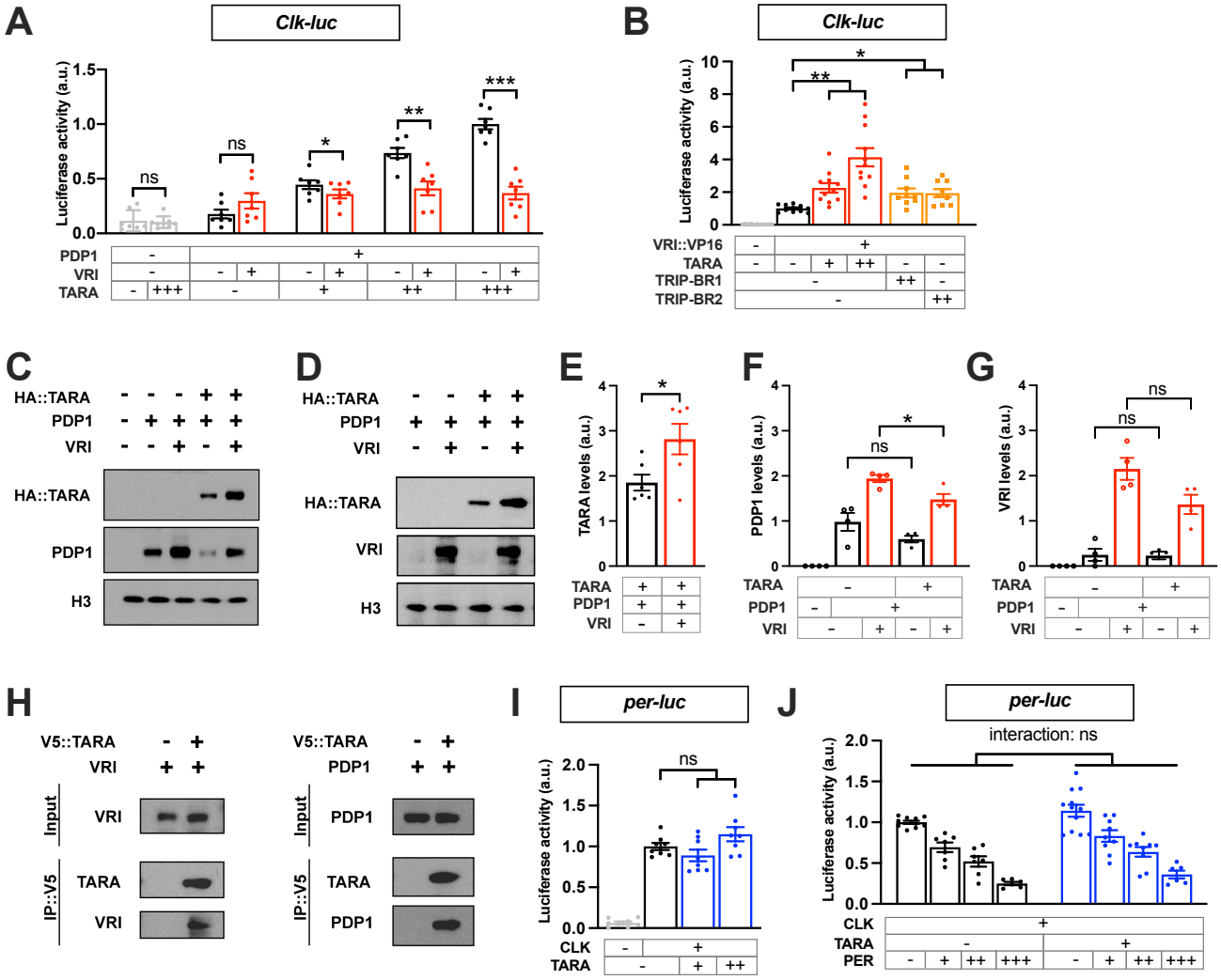
A
Clk-luc
Luciferase activity (a.u.)
PDP1
VRI
TARA
B
Clk-luc
Luciferase activity (a.u.)
VRI::VP16
TARA
TRIP-BR1
TRIP-BR2
C
HA::TARA
PDP1
VRI
H3
D
HA::TARA
PDP1
VRI
H3
E
TARA levels (a.u.)
TARA
PDP1
VRI
F
PDP1 levels (a.u.)
TARA
PDP1
VRI
G
VRI levels (a.u.)
TARA
PDP1
VRI
H
V5::TARA
VRI
Input
IP::V5
TARA
VRI
V5::TARA
PDP1
Input
IP::V5
TARA
PDP1
I
per-luc
Luciferase activity (a.u.)
CLK
TARA
J
per-luc
interaction: ns
Luciferase activity (a.u.)
CLK
TARA
PER

760

Figure 6

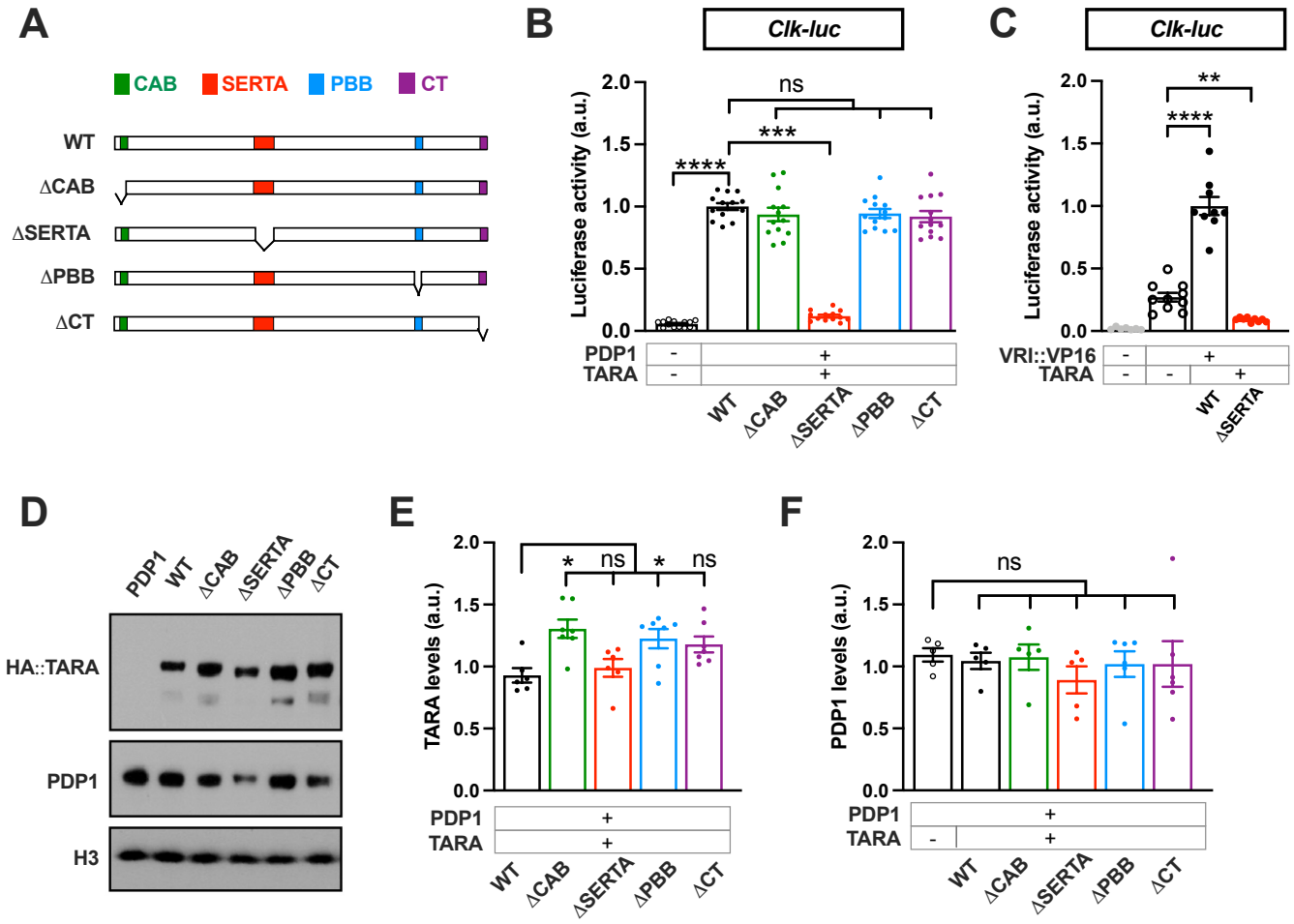
A
CAB
SERTA
PBB
CT
WT
ΔCAB
ΔSERTA
ΔPBB
ΔCT
B
Clk-luc
Luciferase activity (a.u.)
ns
***
****
PDP1
TARA
WT
ΔCAB
ΔSERTA
ΔPBB
ΔCT
C
Clk-luc
Luciferase activity (a.u.)
**
****
VRI::VP16
TARA
WT
ΔSERTA
D
PDP1
WT
ΔCAB
ΔSERTA
ΔPBB
ΔCT
HA::TARA
PDP1
H3
E
TARA levels (a.u.)
*
ns
*
ns
PDP1
TARA
WT
ΔCAB
ΔSERTA
ΔPBB
ΔCT
F
PDP1 levels (a.u.)
ns
PDP1
TARA
WT
ΔCAB
ΔSERTA
ΔPBB
ΔCT

761

Figure 7

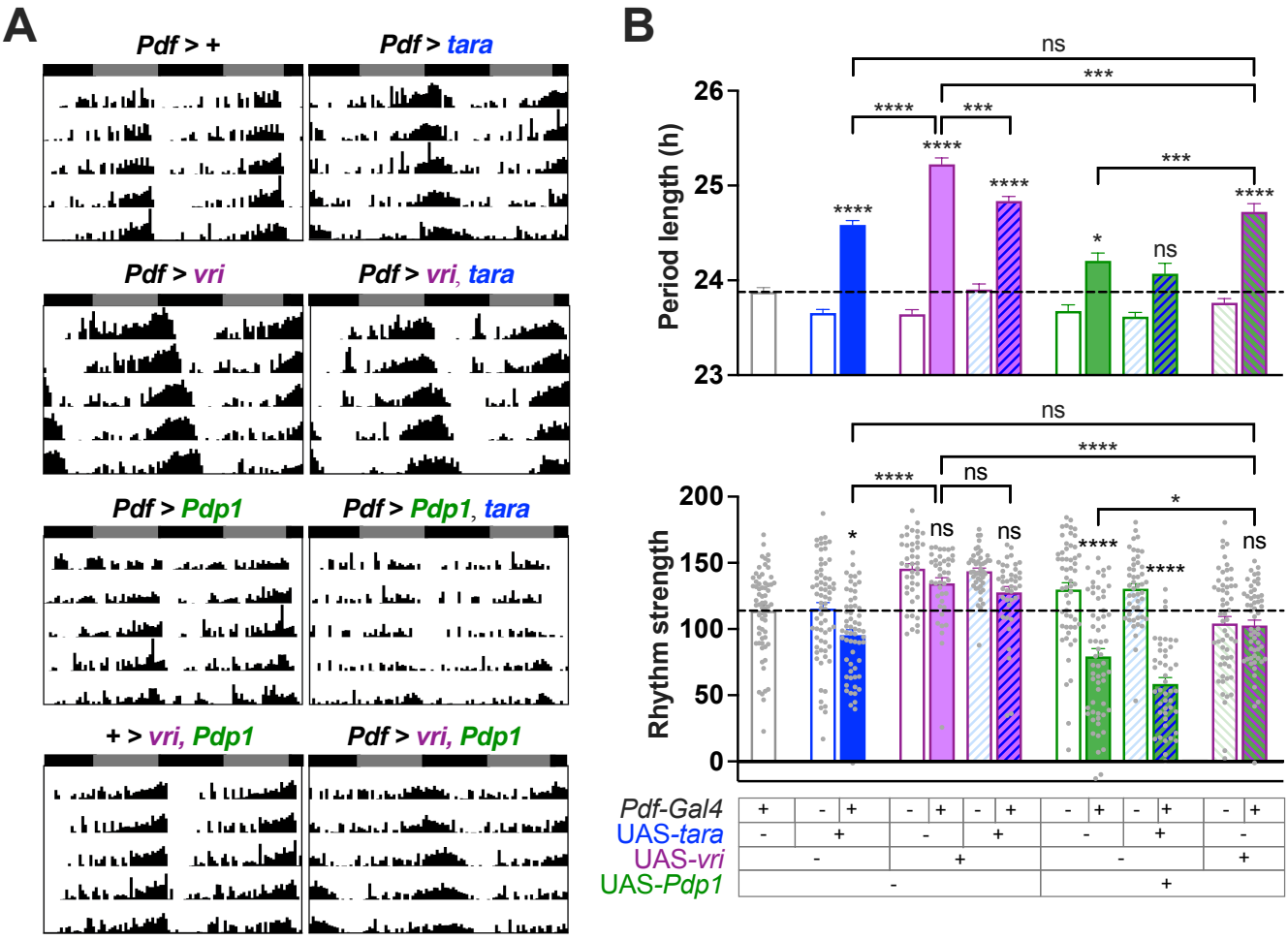
A
Pdf > +
Pdf > tara
Pdf > vri
Pdf > vri, tara
Pdf > Pdp1
Pdf > Pdp1, tara
+ > vri, Pdp1
Pdf > vri, Pdp1
B
Period length (h)
Rhythm strength
Pdf-Gal4
UAS-tara
UAS-vri
UAS-Pdp1

762

763 **Table 1. Circadian locomotor rhythm phenotypes in DD**

Genotype	N	% R	% WR	% AR	tau (h) ± SEM	Power ± SEM
Knockdown						
Female						
+ > *tara* RNAi	63	96.8	1.6	1.6	24.55 ± 0.05	114.1 ± 3.57
elav > +	53	88.7	3.8	7.5	24.31 ± 0.17	98.3 ± 5.14
elav > *tara* RNAi	71	26.8	21.1	52.1	24.03 ± 0.09	30.6 ± 4.86
tim > +	47	83.1	14.8	2.1	24.64 ± 0.05	91.7 ± 5.05
tim > *tara* RNAi	45	60	28.9	11.1	24.36 ± 0.07	62.8 ± 4.90
Pdf > +	29	100	0	0	24.86 ± 0.05	106.0 ± 4.57
Pdf > *tara* RNAi	42	100	0	0	24.79 ± 0.06	114.6 ± 3.32
Male						
+ > *tara* RNAi	38	100	0	0	23.66 ± 0.05	153.6 ± 3.40
tim > +	47	100	0	0	24.39 ± 0.05	135.6 ± 3.23
tim > *tara* RNAi	43	72	14	14	24.26 ± 0.08	69.38 ± 5.90
Pdf > +	31	100	0	0	24.31 ± 0.06	137.6 ± 2.98
Pdf > *tara* RNAi	47	100	0	0	24.09 ± 0.05	131.6 ± 3.04
Overexpression						
Male						
Pdf > +	74	98.6	0	1.4	24.09 ± 0.05	132.6 ± 3.03
+ > *tara*	62	100	0	0	23.97 ± 0.06	130.8 ± 3.09
Pdf > *tara*	54	100	0	0	24.73 ± 0.04	116.3 ± 2.44

764

765 N: number of flies; R: rhythmic; WR: weakly rhythmic; AR: arrhythmic.

766 tau: free-running period; Power: a measure of rhythm strength

767 **Table 2. Circadian locomotor rhythm phenotypes of TARA domain deletion mutants.**

768

Genotype	N	% R	% WR	% AR	tau (h) ± SEM	Power ± SEM
control	28	100	0	0	23.67 ± 0.06	137.0 ± 5.87
ΔCAB	52	71.2	5.8	23.1	23.75 ± 0.07	79.4 ± 8.03
s132/+	66	95.5	1.5	3.0	23.56 ± 0.03	114.7 ± 5.46
s132/ΔSERTA	31	58.1	22.6	19.4	23.63 ± 0.05	56.5 ± 7.76
control	70	97.1	1.4	1.4	23.58 ± 0.03	142.5 ± 4.20
ΔPBB	67	94.0	1.5	4.5	23.61 ± 0.03	121.5 ± 4.39
control	30	96.8	3.2	0	23.54 ± 0.06	134.4 ± 6.59
ΔCT	31	71.6	15.6	12.5	23.56 ± 0.08	85.0 ± 7.57

769 N: number of flies; R: rhythmic; WR: weakly rhythmic; AR: arrhythmic.

770 tau: free-running period; Power: a measure of rhythm strength

771 **Table 3. Circadian locomotor rhythm phenotypes of TARA, VRI, and PDP1**

772 **overexpression in PDF+ neurons**

773

Genotype	N	% R	% WR	% AR	tau (h) ± SEM	Power ± SEM
Pdf > +	64	95.2	3.2	1.6	23.88 ± 0.06	113.8 ± 3.94
+ > *tara*	67	92.5	6	1.5	23.61 ± 0.03	115.3 ± 4.59
Pdf > *tara*	61	93.5	4.9	1.6	24.57 ± 0.05	95.4 ± 4.15
+ > *vri*	42	100	0	0	23.64 ± 0.05	145.6 ± 3.85
Pdf > *vri*	40	97.5	2.5	0	25.23 ± 0.07	134.5 ± 4.21
+ > *vri, tara*	46	100	0	100	23.90 ± 0.06	143.6 ± 2.39
Pdf > *vri, tara*	40	95	5	0	24.84 ± 0.05	127.6 ± 4.50
+ > *Pdp1*	55	96.4	1.8	1.8	23.68 ± 0.07	129.8 ± 5.22
Pdf > *Pdp1*	59	67.8	18.6	13.6	24.21 ± 0.08	79.4 ± 5.81
+ > *Pdp1, tara*	47	97.9	2.1	0	23.62 ± 0.04	130.4 ± 3.79
Pdf > *Pdp1, tara*	44	59.1	22.7	18.2	24.07 ± 0.11	58.5 ± 4.80
+ > *Pdp1, vri*	56	93	3.5	3.5	23.76 ± 0.04	104.3 ± 5.27
Pdf > *Pdp1, vri*	55	94.6	3.6	1.8	24.72 ± 0.09	102.7 ± 4.16

774

775 N: number of flies; R: rhythmic; WR: weakly rhythmic; AR: arrhythmic.

776 tau: free-running period; Power: a measure of rhythm strength.